Physiologia Plantarum
An International Journal for Plant Biology

Physiologia Plantarum 166: 848–861. 2019 ISSN 0031-9317

Roles of plasma membrane proton ATPases AHA2 and AHA7 in normal growth of roots and root hairs in *Arabidopsis thaliana*

Robert D. Hoffmann†, Lene I. Olsen†, Chukwuebuka V. Ezike†, Jesper T. Pedersen†, Raffaele Manstretta, Rosa L. López-Marqués and Michael Palmgren*

Department of Plant and Environmental Sciences, University of Copenhagen, DK-1871, Frederiksberg, Denmark

Correspondence
*Corresponding author,
e-mail: palmgren@plen.ku.dk

Received 22 June 2018;
revised 14 September 2018

doi:10.1111/ppl.12842

Plasma membrane H^+-ATPase pumps build up the electrochemical H^+ gradients that energize most other transport processes into and out of plant cells through channel proteins and secondary active carriers. In *Arabidopsis thaliana*, the AUTOINHIBITED PLASMA MEMBRANE H^+-ATPases AHA1, AHA2 and AHA7 are predominant in root epidermal cells. In contrast to other H^+-ATPases, we find that AHA7 is autoinhibited by a sequence present in the extracellular loop between transmembrane segments 7 and 8. Autoinhibition of pump activity was regulated by extracellular pH, suggesting negative feedback regulation of AHA7 during establishment of an H^+ gradient. Due to genetic redundancy, it has proven difficult to test the role of AHA2 and AHA7, and mutant phenotypes have previously only been observed under nutrient stress conditions. Here, we investigated root and root hair growth under normal conditions in single and double mutants of *AHA2* and *AHA7*. We find that AHA2 drives root cell expansion during growth but that, unexpectedly, restriction of root hair elongation is dependent on AHA2 and AHA7, with each having different roles in this process.

Introduction

Besides anchoring the plant to the ground, roots carry out many essential processes such as mobilization and uptake of nutrients from the soil, where highly controlled growth of the root is also required in order to respond to the nutrient content of the soil. Plasma membrane H^+-ATPases in the root are considered to play essential roles in these processes (Palmgren 2001, Sondergaard et al. 2004, Duby and Boutry 2009). By extruding protons from the root, they acidify the rhizosphere, and through cation exchange they mobilize cations bound to negatively charged soil particles. The membrane potential generated combined with the pH gradient across the plasma membrane constitute the proton motive force that drives uptake of nutrients through channel proteins and proton-coupled secondary active transport systems (Poole 1978, Hedrich and Schroeder 1989). Root growth depends on coordinated expansion of cells, a process that requires local loosening of the cell

Abbreviations – *ACT2*, *ACTIN 2*; *AHA*, *AUTOINHIBITED H^+-ATPASE*; XSEDE, Extreme Science and Engineering Discovery Environment; ICP-OES, inductively coupled plasma optical emission spectrometry; JGI, Joint Genome Institute; LOMETS, Local Meta-Threading-Server.

†These authors equally contributed to this work.

wall matrix followed by uptake of water, and formation and elongation of root hairs. Root hairs are outgrowths of epidermal cells that help to increase the surface area of these absorbing cells, and growth of both roots and root hairs are processes considered to be dependent on plasma membrane H^+-ATPases (Gilroy and Jones 2000, Wang et al. 2007).

In the model plant *Arabidopsis thaliana* (Arabidopsis), 11 *AUTOINHIBITED H^+-ATPASE* (*AHA*) genes encode for plasma membrane H^+-ATPases (Axelsen and Palmgren 2001). AHA1 and AHA2 are the predominant plasma membrane H^+-ATPases (Harper et al. 1989, Pardo and Serrano 1989, Harper et al. 1990). AHA1 is a housekeeping protein found all over the plant, whereas AHA2 plays its major role in the roots. In addition to AHA1 and AHA2, AHA7 is also found in roots (Santi and Schmidt 2009). AHA7 shows a very distinct expression in root hairs (Lan et al. 2013), but is also expressed in pollen tubes (Becker et al. 2014), which, like root hairs, are tip growing structures. AHA2 has a more widespread distribution in roots but is also found in root hairs (Młodzińska et al. 2015). Mutants in these three genes are therefore useful for genetically testing the importance of plasma membrane H^+-ATPases in root nutrient uptake, development and growth.

Genetically testing the roles of *AHA1* and *AHA2* is highly complicated by the fact that knocking out both genes simultaneously results in embryo lethality (Haruta et al. 2010). Mutations in each of the genes result in plants with no apparent phenotypes unless the mutant plants are challenged, which suggests redundant function of these two genes. Compared to wild-type plants, *aha2* knockout plants are more tolerant to toxic cations such as cesium and lithium, which is evidence that in *aha2* plants the plasma membrane electric potential is reduced (Haruta and Sussman 2012). A knockout of *AHA7* produces no apparent phenotype under normal growth conditions but, under conditions of iron and phosphate scarcity root hair initiation is challenged (Santi and Schmidt 2009, Yuan et al. 2017).

While previous research has pointed to important roles for root plasma membrane H^+-ATPases under stress conditions where the supply of specific nutrients is limiting, they do not answer the question as to whether *AHA* genes are required for normal growth of roots and root hairs. As explained above, gene redundancy hampers investigation of this question. In this work, we took a closer look at AHA7 and investigated the biochemical properties of the recombinant protein to learn whether it has specific properties that could be used to predict functional roles of the protein in planta. Subsequently, and under normal growth conditions, we analyzed the phenotypes of *aha7* and *aha2* as well as *aha2 aha7* double mutant plants. We report that AHA7 is a plasma membrane H^+-ATPase with unusual biochemical properties and that it accelerates the growth rate of root hairs when *AHA2* is lacking.

Materials and methods

Identification of plasma membrane H^+-ATPase sequences

The strategy used to identify sequences was as previously reported (Palmgren et al. 2017). Sequences of plant plasma membrane H^+-ATPases were identified using the Basic Local Alignment Search Tool (BLAST) program (http://blast.ncbi.nlm.nih.gov/) to search the genomes of plant species representing major evolutionary stages. For each species, BLAST searches were carried out using the *A. thaliana* AHA7 (Q9LY32) and AHA2 (P19456) amino acid sequences. Additional searches for homologs were carried out through BLAST searches at the Joint Genome Institute (JGI) Genome Portal (http://genome.jgi.doe.gov/), the Kyoto Encyclopedia of Genes and Genomes (KEGG; https://www.genome.jp/kegg/), the Phytozome Plant Genomics Resource (https://phytozome.jgi.doe.gov/pz/portal.html#!search?show=BLAST), the Conifer Genome Network Dendrome Database (http://dendrome.ucdavis.edu/resources/blast/) and the Plant morphogenesis server (http://www.plantmorphogenesis.bio.titech.ac.jp/~algae_genome_project/klebsormidium/klebsormidium_blast.html). All hits in each species with significant similarity to the query (expected value of $<e^{-30}$) were selected and their relationship to plasma membrane H^+-ATPases was investigated by constructing phylogenetic trees for all candidate sequences in each individual genome together with a set of known P-type ATPases using MUSCLE alignment (Edgar 2004) and then maximum likelihood phylogeny reconstruction in a Gamma distributed LG model (Le and Gascuel 1993) as identified by ProtTest (Abascal et al. 2005) and implemented in MEGA6 (Tamura et al. 2013). The nature of the individual sequences was subsequently confirmed by manual inspection for conserved sequence motifs characteristic of P-type P3A pumps (Buch-Pedersen et al. 2009).

Phylogenetic analysis of P-type ATPases

Protein sequence alignment was performed using MUSCLE (Edgar 2004) implemented in MEGA6. This resulted in a total of 1059 positions (43 amino acid sequences) in the data set of plant plasma membrane H^+-ATPases. The evolutionary history was inferred assuming an LG + INVGAMMA model (see above). Phylogenetic analyses were subsequently conducted using Bayesian

inference as performed with MrBayes 3.2.2 (Ronquist and Huelsenbeck 2003). MrBayes analysis was performed using the following settings: eight chains of Markov chain Monte Carlo iterations and heated parameter of 0.05 with trees sampled every 1000 generations. The average SD of split frequencies at termination of the analysis after 2 000 000 generations were 0.002612 for the phylogenetic tree in Fig. 2B. The MrBayes analysis was run on the CIPRES Science Gateway (Miller et al. 2010) in the Extreme Science and Engineering Discovery Environment (XSEDE).

Structural modeling

A prediction of the structure of AHA7 was obtained using the online web service for protein structure prediction Local Meta-Threading-Server (LOMETS). 3D models were generated by collecting high-scoring target-to-template alignments from nine locally installed threading programs (FFAS, HHsearch, MUSTER, PPA, PRC, PROSPECT2, SAM-T02, SP3 and SPARKS). From the 10 obtained outputs, a high-score prediction was made on the structure of AHA2 (Pedersen et al. 2007). The obtained structure was then further analyzed with the molecular visualization system PyMol.

Plant lines

Seeds for *aha7*-1 (SALK_042485) and *aha7*-2 (SALK_105742C; Santi and Schmidt 2009), and *aha2-4* (Haruta et al. 2010) were ordered from the European Arabidopsis Stock Centre, NASC.

Plant growth conditions

The growth media for Arabidopsis grown on plates was made following the protocol of Santi and Schmidt (2009) and contained 5 mM KNO_3, 2 mM $MgSO_4$, 2 mM $Ca(NO_3)_2$, 2.5 mM KH_2PO_4, 70 μM H_3BO_3, 14 μM $MnCl_2$, 1 μM $ZnSO_4$, 0.5 μM $CuSO_4$, 10 μM NaCl, 0.2 μM Na_2MoO_4 and 50 μM Fe-EDTA, solidified with 0.3% Phytagel (Sigma-Aldrich, Saint Louis, MO). Sucrose (43 mM) and 4.7 mM 2-(N-morpholino)ethanesulfonic acid (MES) were included and the pH was adjusted to 5.5 with KOH. Where applicable, 50 mg ml^{-1} hygromycin B were added. The preparation of plates with Murashige–Skoog medium (Murashige and Skoog 1962) as described by Haruta et al. (2010). Arabidopsis seeds were surface sterilized by washing them with 70% ethanol for 10 min, bleach solution with 0.05% Tween-20 for 5 min, 70% ethanol for 5 min, followed by rinsing three times in sterile milliQ water. Seeds were plated and the plates stored at 4°C for 48 h. Plants on plates or soil were grown in growth chambers at 20°C with 16 h light period (120 μmol photons m^{-2} s^{-1}).

Measurements of root hairs

Images of roots were captured using a Leica MY FLII stereo microscope, and ImageJ software was used to measure the length of root hairs within 10 mm, starting 5 mm away from the root tip.

In vitro pollen tube growth

Newly opened flowers were collected and carefully dipped onto microscope slides covered with solidified pollen germination medium (5 mM $CaCl_2$, 5 mM KCl, 1 mM $MgSO_4$, 0.01% H_3BO_3, 15% sucrose, 1.25% low melting agarose, pH 7.5). A cover glass was placed on the pollen grains and slides were incubated for 3 h in a humid chamber inside an incubator set to 22°C (Boavida and McCormick 2007).

Construction of the fluorescent fusion *pAHA7::AHA7::*green fluorescent protein

Genomic *A. thaliana* Col-0 DNA was amplified by Phusion high-fidelity DNA-polymerase (New England BioLabs, Ipswich, MA) using primer pairs that included 1534 bp upstream of the start codon and the entire gene, only omitting the stop codon (Table S3, Supporting Information). The resulting polymerase chain reaction (PCR) product was cloned into the pENTR/D-TOPO vectors (Invitrogen, Carlsbad, CA) by TOPO-cloning, according to the manufacturer's instructions, and the insert was fully sequenced. Using LR recombinase (Invitrogen), the insert was subsequently transferred into destination vector pMDC107 (Curtis and Grossniklaus 2003).

Construction of the *pAHA7::*glucuronidase construct

Genomic *A. thaliana* Col-0 DNA was used as a template for PCR using Phusion high-fidelity DNA polymerase (New England Biolabs, Ipswich, MA) and using primer pairs that included 1534 bp upstream of the start codon and 168 bp of *AHA7*, extending into the second exon (Table S2). The resulting PCR product was cloned into the pENTR/D-TOPO vectors (Invitrogen) by TOPO-cloning, according to the manufacturer's instructions, and the insert was fully sequenced. Using LR recombinase (Invitrogen), the insert was subsequently transferred into destination vector pMDC162 (Curtis and Grossniklaus 2003).

Plant transformation

Plasmids were transformed by electroporation into *Agrobacterium tumefaciens* strain GV3101::pMP90

(Koncz and Schell 1986) and transformants were selected on YEP plates (1% yeast extract, 1% Bacto Peptone, 0.5% NaCl and 1.5% Bacto Agar) containing 50 mg ml^{-1} kanamycin and 25 mg ml^{-1} gentamycin. Destination vectors extracted from *A. tumefaciens* single colonies were sequenced to verify the inserts. *Arabidopsis thaliana* plants were transformed with *A. tumefaciens* (strain GV3101::pMP90) containing the desired vectors. For plant transformation, a modified protocol of the floral-dip method was used (Logemann et al. 2006). Briefly, *A. tumefaciens* cells were grown on three plates containing YEP, 50 mg ml^{-1} kanamycin and 25 mg ml^{-1} gentamycin for 48 h. Cells were then resuspended in 150 ml infiltration solution containing 5% sucrose (w/v) and 0.03% Silwet L-77 (Lehle seeds, Round Rock, TX). Inflorescences of newly bolted Arabidopsis (Col-0) plants were dipped into the infiltration solution for 30 s and subsequently covered with a plastic bag over night. This was repeated three times, allowing the plants to recover for 5–7 days in between.

Selection of transformed plants

Seeds of infiltrated plants were surface sterilized by washing them with 70% ethanol for 10 min, bleach solution with 0.05% Tween-20 for 5 min, 70% ethanol for 5 min, followed by rinsing three times in milliQ water. Seeds were plated on 1/2 strength MS medium supplemented with 1% sucrose (w/v) and 50 mg ml^{-1} hygromycin B. After storing the plates at 4°C for 48 h, they were transferred to growth chambers at 20°C with 16 h light period (120 µmol photons m^{-2} s^{-1}). After 2 weeks, seedlings showing resistance to hygromycin B were transferred to soil and tested by PCR for the presence of the correct insert.

GUS staining and analysis

To determine the tissue-specific expression of *AHA7*, 7-days old plate-grown seedlings were stained for GUS activity. Samples were vacuum infiltrated for 5 min with 5-bromo-4-chloro-3-indolyl β-D-glucuronic acid (X-GlcA; Duchefa, Haarlem, Netherlands) solution containing 3 mM $K_3(Fe(CN)_6)$, 3 mM $K_4(Fe(CN)_6)$, 0.4% Tween-20, 50 mM KH_2PO_4/K_2HPO_4 pH 7.2, 2 mM X-GlcA and incubated in the solution at 37°C in the dark for 3 h. Bright-field images of the seedlings were acquired with a Leica DM 5000B microscope (Leica, Wetzlar, Germany).

Confocal imaging

Seeds of *aha7-2* plants complemented with an *AHA7–Enhanced GFP (EGFP)* construct expressed under *AHA7* promoter were analyzed. For root hair imaging, 7-days old seedlings were analyzed using a Leica TCS SP5-X confocal laser scanning microscope (CLSM) and a 63× HCX PL APO [numerical aperture (NA) 1.2 water; Leica Microsystems, Wetzlar, Germany] objective. Image acquisition was done using excitation with 488 nm argon laser line and acquiring the emission pattern of Enhanced GFP (GFP) between 500 and 560 nm. For pollen tubes, images were obtained with a Leica SP5, using a 40× HCX PL APO (NA 0.75–1.25 oil; Leica Microsystems) objective (NA 1.0; Leica). EGFP was excited with the 488 nm line of an argon laser and emission recorded from 500 to 560 nm. Optical sections were captured and images were prepared by generating max-intensity projections (using ImageJ) of the optical sections through an individual pollen tube. Auto fluorescence (monitored in wild-type mature pollen and pollen tubes) was negligible in comparison with pollen expressing EGFP.

Construction of *AHA7* full length and *AHA7* C-terminally truncated cDNA constructs

Total RNA was extracted from Arabidopsis Col-0 seedlings using Plant RNAeasy kit (Qiagen, Hilden, Germany) according to the manufacturer's instructions. To synthesize cDNA, 1 mg RNA was reverse transcribed using the iScript cDNA Synthesis Kit (Bio-Rad, Hercules, CA) according to the manufacturer's instructions. The PCR products of *AHA7* full length coding sequence and *aha7* C-terminally truncated sequence (see Table S2 for primer sequences) were cloned into the pENTR/D-TOPO vectors (Invitrogen) by TOPO-cloning, according to the manufacturer's instructions, and the inserts were fully sequenced. Using LR recombinase (Invitrogen), the inserts were subsequently transferred into destination vector pMP4409. pMP4409 was generated by cutting pMP625 containing the promoter and terminator of *PMA1* (yeast endogenous plasma membrane H^+-ATPase; Villalba et al. 1992) with *Xho*I and *Spe*I, removing *AHA2*, followed by inserting Gateway Cassette A (Invitrogen); the correct orientation of the Gateway Cassette A was verified by sequencing.

Construction of *aha7Δ92ΔEL*

The pENTR/D-Topo vector containing *aha7Δ92* was used as template to create *aha7Δ92ΔEL*, which has the sequence between TM7 and TM8 substituted with the corresponding sequence of *AHA2*. This substitution was obtained by overlapping PCR (see Table S2 for primer sequences).

Yeast complementation assay

pMP4409 plasmids containing *AHA7* full length cDNA, *aha7*Δ*92*, *aha7*Δ*92*ΔEL, *AHA2* full length or *aha2*Δ*92* as positive control were transformed into *Saccharomyces cerevisiae* strain RS-72 (*Mat a; ade1-100 his4-519 leu2-3, 312 pPMA1-pGAL1*) to be used for complementation tests as described previously (Buch-Pedersen et al. 2003). Each complementation experiment was replicated independently three times. In drop tests, cells were diluted in sterile water to an optical density of 0.1 and 0.01, respectively, and 5 µl droplets were spotted on selective media.

Protein expression, purification and biochemical characterization

Transformed yeast cells were grown and the microsomes isolated as described previously (Wielandt et al. 2015). The ATPase activity was determined by assaying liberation of phosphate according to the Baginski assay (Baginski et al. 1967) and assayed in microtiter plates with a total volume of 60 µl in a buffer containing 50 mM MOPS/MES, 8 mM $MgSO_4$, 5 mM NaN_3, 0.25 mM $NaMoO_4$, 25 mM KNO_3, 2 mM phosphoenolpyruvate and 30 µg ml^{-1} pyruvate kinase from rabbit muscle (Sigma-Aldrich, St Louis, MO). The assay buffers were equilibrated to 30°C, and the assays were started by adding ATP and 150 ng isolated microsomes. The ATPase activity was measured in a pH range from 5.4 to 8.1 and with 3 mM ATP when determining the pH optima. For kinetic characterization of the ATPase activity, the pH was constant at 6.5 and 12 ATP concentrations were tested in the range 0–3 mM. All experiments were performed in triplicates with ±SE.

Sodium dodecyl sulfate polyacrylamide gel (SDS-PAGE) electrophoresis was performed according to standard techniques. Then, 8 µg total microsomes were loaded in each lane and relative plasma membrane H^+-ATPase expression levels in total microsomes were estimated using ImageJ and their gel analyzing tool (Schneider et al. 2012).

Hydroponic growth

Seeds of wild-type and *aha2* were germinated in water for 1 week, followed by 4 weeks in hydroponics media with 8 h light. In the first 2 weeks, the media contained 2.5 mM KNO_3, 1 mM $MgSO_4$, 1.25 nM KH_2PO_4, 1 mM $Ca(NO_3)_2$, 35 µM H_3BO_3, 7 µM $MnCl_2$, 0.5 µM $ZnSO_4$, 0.25 µM $CuSO_4$, 5 µM NaCl, 0.1 µM Na_2MoO_4 and 25 µM FeEDTA, pH was adjusted to 5.7 using KOH. For the last 2 weeks, the media was concentrated 2X with an identical pH. The hydroponic medium was changed three times a week. The 5-weeks-old plants were separated into rosette and roots, root length and rosette area were calculated. Roots were desorbed in ice-cold 0.1 M $CaCl_2$ with 10 mM EDTA for 10 min, rinsed twice in MilliQ water, and stored at −80°C until used for analysis.

Inductively coupled plasma optical emission spectrometry element analysis

Roots and rosettes from wild-type and *aha2* grown hydroponically were freeze dried. Following recording of dry weights, inductively coupled plasma optical emission spectrometry (ICP-OES) analysis was performed as described previously (Olsen et al. 2016).

qPCR analysis

In this section, 7-days-old wild-type and *aha2* seedlings (grown on plates with Hoagland medium under 16 h light conditions) were separated into leaves and roots, frozen in liquid nitrogen and saved at −80°C. RNA from roots was extracted using the E.Z.N.A Plant RNA Kit (Omega Bio-Tek, Doraville, CA) and DNase treated using the Turbo DNase Free Kit (Ambion, Austin, TX). cDNA was synthesized using the iScript cDNA Synthesis Kit (Bio-Rad, Hercules, CA). The real-time quantitative PCR were run on the Agilent Mx3005P using Agilent Brilliant II SYBR Green (Agilent, Santa Clara, CA) with the following program: 95°C for 10 min followed by 40 cycles of 95°C for 15 s, 59°C for 30 s and 72°C for 30 s. Gene expression was normalized to *ACTIN 2* (*ACT2*) and *UBIQUITIN 21* (*UBC21*). Data represent six biological replicates, each with three technical replicates. Quantitative PCR (qPCR) primers used in this study can be found in Table S3.

Results and discussion

AHA7 is expressed in tip-growing cells

To investigate the tissue specific expression of *AHA7* in more detail, the promoter region of *AHA7* was fused to the GUS reporter gene and transgenic plants expressing this construct were generated. In these plants, GUS activity was absent from leaves and stems but was high in root hairs and pollen grains (Fig. 1A, B). After fusing the promoter and coding region of the *AHA7* gene with GFP, we found that the signal of GFP-tagged AHA7 in root hair cells was strongest at the root hair bulging site and at the growing root hair tip (Fig. 1C, D). Because AHA7 is also expressed in pollen, we assessed AHA7::GFP localization in growing pollen tubes and found that AHA7::GFP in pollen tubes was absent from the growing

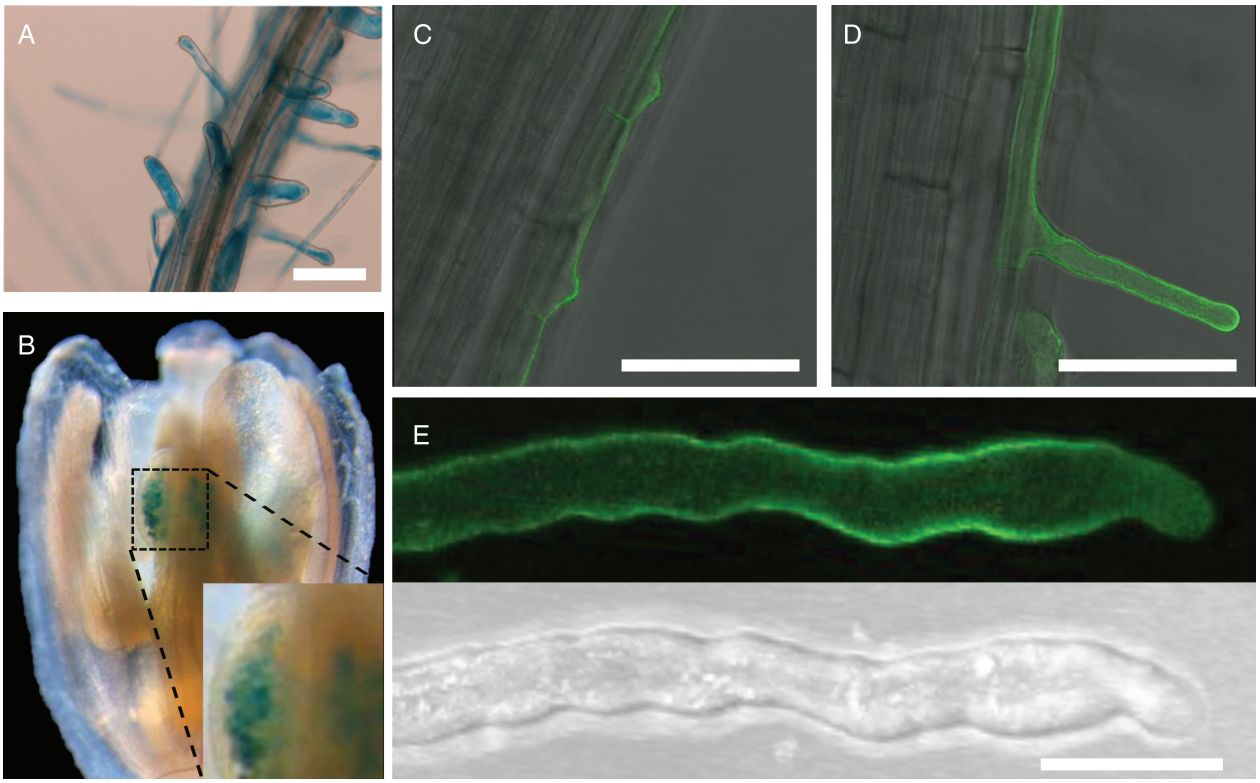

Fig. 1. Localization of AHA7 in root hairs is different from that in pollen tubes. *AHA7* promoter-driven expression of the *GUS* reporter gene shows specific expression in root hairs (A) and pollen grains (B). (C) *AHA7* promoter-driven expression of an *AHA7::GFP* fusion protein confirms expression in root hairs and shows strong fluorescence signal in the plasma membrane at the root hair bulging site. (D) In growing root hairs, AHA7::GFP localizes to the apex of the growing tip. (E) *AHA7* promoter-driven expression of an *AHA7::GFP* fusion protein in pollen tubes shows localization of AHA7 to the plasma membrane in the region behind the growing tip apex (*z*-projection of max intensity). Scale bars in A, C and D represent 100 μm, in E 10 μm.

tip membrane (Fig. 1E). A similar expression pattern where a plasma membrane proton pump was excluded from the growing pollen tube tip has been described in tobacco (Certal et al. 2008). The fact that AHA7 is present in the tip of growing root hair cells but excluded from the tip of growing pollen tubes suggests that tip growth in root hairs and pollen tubes underlies different molecular programs, as hypothesized before (Schoenaers et al. 2017), and indicates that AHA7 plays different roles in these two programs.

AHA2 and AHA7 group into different phylogenetic clades

A phylogenetic analysis of plant plasma membrane H^+-ATPase sequences revealed that they divide into two major monophyletic clades (labeled a and b in Fig. 2A), with AHA2 and AHA7 in clades a and b, respectively. There were two differentiators between the two clades. First, compared to plasma membrane H^+-ATPase sequences in clade a, sequences in clade b had an insert of 4–13 residues in an extracellular loop between transmembrane segments 7 and 8 (Fig. 2B, C). Second, the C-terminus of plasma membrane H^+-ATPases harbors two autoinhibitory amino acid stretches, regions I and II (Axelsen et al. 1999; Fig. S1). The C-terminal domains of AHA2 and AHA7 are very similar albeit pumps in clade b harbor a conserved negatively charged residue (Glu) in region II not found in pumps of clade a, and AHA7 and related pumps has an additional Glu in region I (Fig. S1). Sequences of the moss *Physcomitrella patens* were abundant at the base of clade a and at the root of the tree, where they group together with that of the charophyte *Klebsormidium flaccidens* but were absent from clade b (Fig. 2A). This would suggest that AHA2 is related to the first plasma membrane H^+-ATPases of land plants, whereas AHA7 evolved with appearance of vascular plants with a root system.

AHA7 is inhibited by acidic extracellular pH

To confirm that AHA7 encodes a functional proton pump, the gene was put under control of the strong constitutive promoter of the *S. cerevisiae* plasma membrane

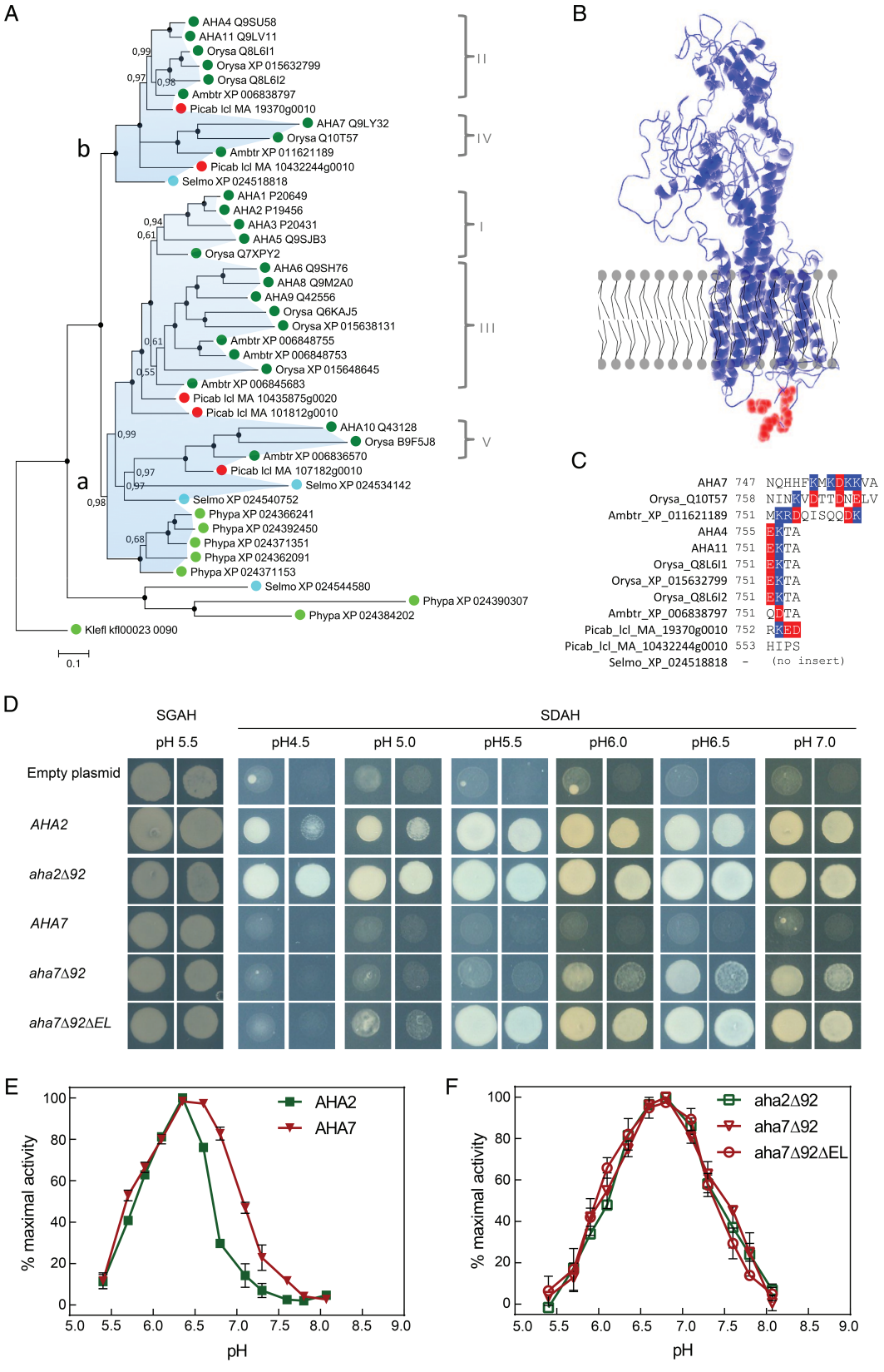

Fig. 2. Legend on next page.

H^+-ATPase *PMA1* and expressed in the yeast strain RS-72 in which the expression of *PMA1* is turned off on glucose medium. As plant plasma membrane H^+-ATPases require posttranslational neutralization of their C-terminal autoinhibitory regulatory domain to be fully active, we truncated at the gene level the C-terminal 92 amino acid residues of AHA7 (to create aha7Δ92). When transferred to plates with glucose as carbon source, yeast cells expressing C-terminally deleted *AHA7* complemented *pma1*, but complementation was only possible when the pH of the external medium was close to neutral (Fig. 2D). Thus, *AHA7* was not able to complement *pma1* and drive yeast growth when external pH was below pH 6.0. In contrast, the related and well-characterized plasma membrane H^+-ATPase *AHA2*, readily complemented *pma1* even at an external pH of 4.5.

AHA7 is autoinhibited by an extracellular loop

As neither full-length AHA7 nor the C-terminally truncated pump could complement growth of *pma1* mutant at pH below 6, we deleted in addition the loop in AHA7 by site-directed mutagenesis to make it resemble the sequence of AHA2. The resulting mutant pump (aha2Δ92ΔEL) was indeed able to complement *pma1* at pH 5.5 (Fig. 2D). This suggests that at acidic extracellular pH the extracellular loop plays a role in inhibiting proton pumping of AHA7. The extracellular loop in sequences of clade b is only weakly conserved in land plants but always contains an acidic residue (Fig. 2C), which suggests that inhibition is the result of protonation of an acidic group in the loop. Compared to AHA7 and its homolog in other plants, a similar insert, but shorter (only four residues but one of them negatively charged), was found in the closely related plasma membrane H^+-ATPases AHA4 and AHA11 and their relatives in land plants (Fig. 2C), and it is therefore possible that autoinhibition by an acidic extracellular loop is to be found in other proton pumps in clade b. Root hair tip growth is tightly associated with oscillatory changes in surface pH (Monshausen et al. 2007). Since AHA7, in contrast to AHA2, cannot sustain yeast growth when growth medium gets below pH 6.0, it suggests a mechanism by which AHA7 could contribute to generating oscillating proton fluxes during root hair tip growth.

Using isolated microsomal membranes, the biochemical properties of the AHA7 protein expressed in yeast could be analyzed. As expected, the ATP affinity of AHA7 did increase when the autoinhibitory C-terminus was removed (measured as a decrease in K_m for ATP; Table 1). The maximal ATP hydrolytic activity (V_{max}) was almost unaffected by C-terminal removal and remained three to four times lower than that of AHA2 and aha2Δ92. However, when the extracellular loop in aha7Δ92 was removed, V_{max} increased about 7-fold and reached approximately the same value as that of aha2Δ92, indicating that the extracellular loop in AHA7 inhibits ATP turnover. The relative protein expression levels of AHA2 and AHA7, and aha2Δ92 and aha7Δ92ΔEL were estimated and showed that the lower catalytic activity of full-length AHA7 is not due to low expression levels in yeast (Fig. S2). These results suggest that the basic machineries of AHA2 and AHA7 are identical, but that they differ in their mode of regulation.

AHA7 and AHA2 respond differently to changes in cytoplasmic pH

Plasma membrane H^+-ATPase pump activity in response to changes in cytoplasmic pH reflects the affinity of

Fig. 2. AHA7 activity is controlled by apoplastic pH. (A) Phylogenetic tree showing that AHA7 evolved with appearance of vascular plants with a root system. Two major clades of land plant sequences are highlighted (labeled a and b, respectively). Roman numerals indicate the previous nomenclature for angiosperm clades of plasma membrane H^+-ATPases (Palmgren 2001). In the tree, Bayesian probabilities are indicated at nodes. Black circles at nodes indicate maximum statistical support (Bayesian probability = 1). Accession codes for protein sequences used for building the tree are indicated. Abbreviations are: AHA, autoinhibited H^+-ATPase from *Arabidopsis thaliana* (Dicotyledonae); Orysa, *Orysa sativa* (Monocotyledonae); Ambtr, *Amborella trichopoda* (basal angiosperm); Picab, *Picea abies* (Gymnospermae), Selmo, *Selaginella moellendorffii* (Lycopodiophyta; basal vascular plants); Phypa, *Physcomitrella patens* (Bryophyta; land plants without a vascular system); *Klebsormidium flaccidens* (Charophyta; green algae). (B) AHA7 contains a stretch of charged amino acids in a loop on the extracellular side of the protein facing the apoplast (between transmembrane segments 7 and 8) which is absent from plasma membrane H^+-ATPases in clade a. A model of the AHA7 pump built on the AHA2 crystal structure is shown with the extracellular amino acid stretch marked in red. (C) Plasma membrane H^+-ATPases in clade b contain a stretch of charged amino acid residues between transmembrane segments 7 and 8. An exception is the *S. moellendorffii* sequence at the base of the clade. (D) Complementation of a yeast strain lacking the endogenous plasma membrane H^+-ATPase shows that the extracellular loop between transmembrane segments 7 and 8 is involved in restricting pumping of protons when apoplastic pH is more acidic than pH 6.0. The last 92 C-terminal amino acid residues were truncated at the gene level to relieve the pump's autoinhibition in the heterologous expression system. (E) AHA7 has half maximal ATP hydrolytic activity at pH 7.0 (around cytoplasmic pH) whereas AHA2 is almost inactive at neutral pH. The ATP hydrolytic activity as a function of pH was measured in microsomal membranes of yeast expressing the recombinant protein. (F) When deprived of their regulatory autoinhibitory C-terminal domains, AHA2 and AHA7 have similar ATPase activity profiles as a function of pH. SGAH, synthetic galactose medium supplied with adenine and histidine. SDAH, synthetic dextrose (glucose) medium supplied with adenine and histidine.

Table 1. Kinetic parameters of AHA2 and AHA7 plasma membrane H^+-ATPases expressed in microsomal membranes of *Saccharomyces cerevisiae*. n = 3 (biological replicates). rel, relative. [a]In mM; [b]In μmol P_i min^{-1} mg^{-1} microsomal membrane protein; [c]In % relative to the expression level of recombinant AHA2 in yeast microsomal membranes; [d]In % relative to the V_{max} of AHA2.

Protein	K_m (ATP)[a]	V_{max}[b]	Expression level (rel)[c]	V_{max} (rel)[d]
AHA2	1.3 ± 0.3	1.5 ± 0.1	100	1.0
aha2Δ92	0.4 ± 0.1	2.0 ± 0.2	41 ± 4	3.3 ± 0.4
AHA7	1.4 ± 0.3	0.5 ± 0.1	97 ± 13	0.4 ± 0.2
aha7Δ92	0.4 ± 0.1	0.6 ± 0.1	56 ± 11	0.7 ± 0.2
aha7Δ92ΔEL	0.5 ± 0.1	2.0 ± 0.2	35 ± 4	3.8 ± 0.4

the pump for H^+ entering from the cytoplasmic side (Buch-Pedersen et al. 2009). The ATP hydrolytic activity of AHA7 as a function of pH revealed that its activity was half-maximal at pH 7 (Fig. 2E), which is approximately the pH of the cytoplasm. This is in contrast to AHA2, which has very low activity at cytoplasmic pH but is strongly activated at more acidic pH with an optimum at pH 6.4 (Fig. 2E). Deletion of the AHA2 C-terminal end resulted in a shift of the optimal pH from approximately pH 6.3–6.8, confirming previous results (Buch-Pedersen et al. 2009). However, almost no variation in the optimal pH was found when the C-terminal end of AHA7 was deleted (Fig. 2F), suggesting that the function of the C-terminal domain of AHA7 does not regulate H^+ affinity, but is restricted to regulating the affinity for ATP (Table 1).

Generation of *aha2 aha7* double knockout mutants

To investigate the physiological function of AHA7, we employed two independent Arabidopsis lines, *aha7*-1 and *aha7*-2 (Santi and Schmidt 2009, Yuan et al. 2017), each carrying a T-DNA insertion in the *AHA7* gene. The resulting plants had no apparent phenotype when grown under standard conditions. Plants heterozygous for either *aha7-1* or *aha7-2* produced offspring with a Mendelian distribution of the wild-type and *aha7* alleles (Table S1). We measured root length, root hair density and root hair length and found no statistical significant differences from that of the wild-type. Because AHA2 and AHA7 are needed for proper root hair function (Santi and Schmidt 2009, Yuan et al. 2017), we crossed the *aha7* mutants with a previously characterized knockout mutant of AHA2, *aha2-4*, and allowed the resulting plants to self in order to generate homozygous *aha2 aha7* double mutants.

Root hair growth is increased in *aha2* and *aha2 aha7* knockout mutants

Previously, no phenotypes have been reported for *aha2* or *aha7* mutants when grown under normal growth conditions. However, we found that root hairs in *aha2* and also in *aha2 aha7* double mutants were longer than those of the wild-type (Fig. 3A, B), whereas root hair density was identical (Fig. 3C). Our finding that root hair growth is promoted by the lack of *AHA2* alone and together with *AHA7* is in accordance with the observation that vanadate, which is an inhibitor of P-type ATPases such as the plasma membrane H^+-ATPase, has a strong positive effect on root hair growth (Lin et al. 2015). However, lack of *AHA7* alone had no apparent effect on root hair growth (Fig. 3A, B). We then measured the root hair growth rates. The increase in root hair length of *aha2* was the result of a higher root hair growth rate. By contrast, root hairs of *aha2 aha7* double mutants grew as fast as those of the wild-type, but ceased to grow later, which caused the increase in root hair length observed for these double mutants. Also, we found that root hairs of *aha7* single mutant plants ceased growth later than wild-type. However, while wild-type root hairs grew at a constant rate and stopped growing rather abruptly, root hairs of *aha7* stopped growing gradually, resulting in a final root hair length indistinguishable from that of wild-type (Fig. 3D). Taken together, this suggests that *AHA7* is responsible for the increase in root hair growth rate observed in the absence of *AHA2*. Assuming that lack of the major proton pump AHA2 leads to a less acidified apoplast, this change in extracellular pH would explain why AHA7, which is inhibited by acidic extracellular pH, in turn is activated when AHA2 is absent. The increased root hair growth rate in *aha2* also demonstrates that AHA2-driven acidification of the cell wall is not a prerequisite for root hair growth.

AHA2 influences the length of trichoblast cells

We measured the length of cells in the mature root hair zone and found that, compared to wild-type, the length of trichoblast cells was shorter in the *aha2* mutant (Fig. 4D). This caused the root length of *aha2* seedlings to be shorter than that of the wild-type (Fig. 4A,B). Also, the cotyledons of *aha2* and *aha2 aha7* were smaller than the wild-type (Fig. 4C). This is in contrast to Haruta and

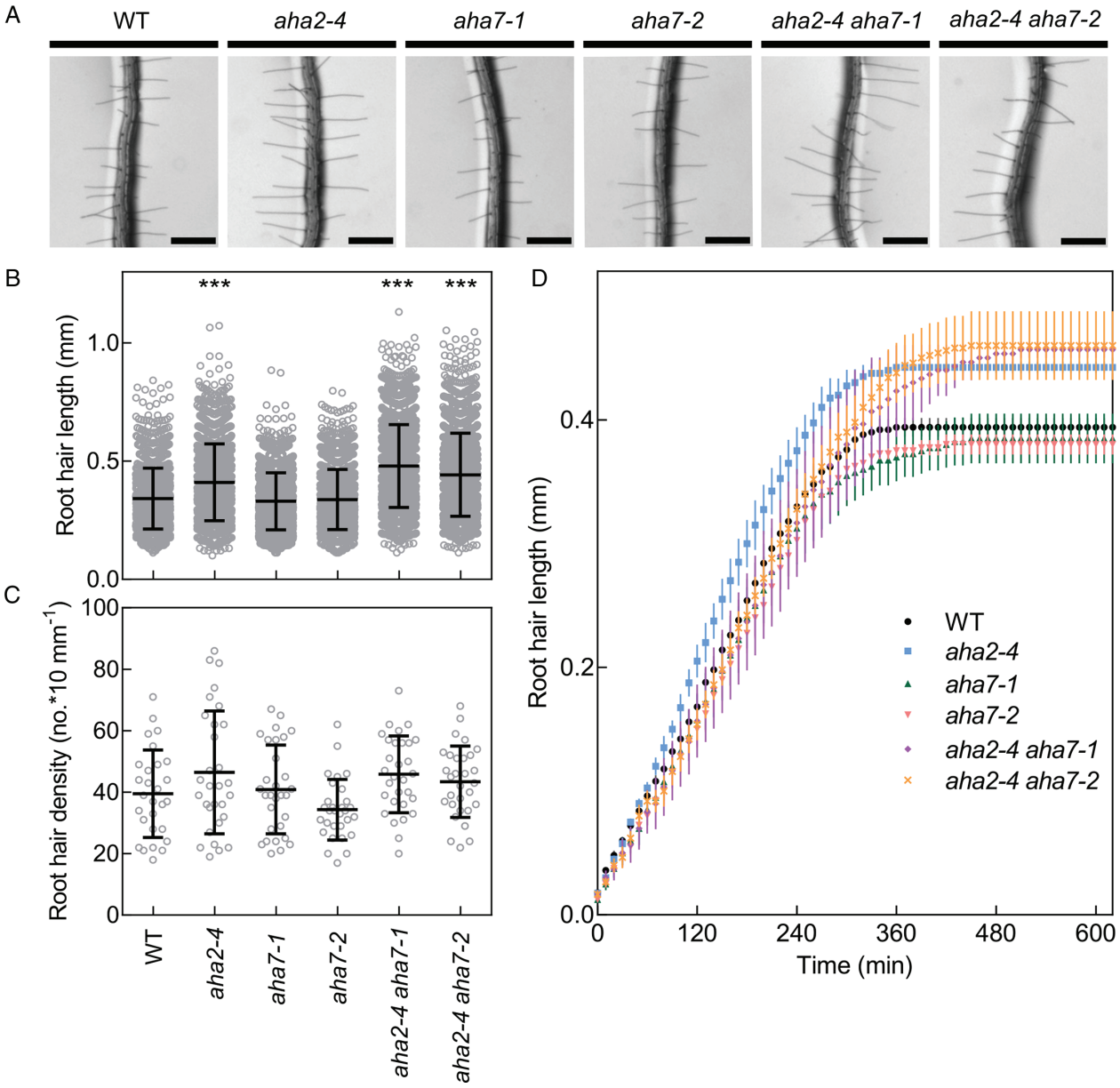

Fig. 3. Root hairs of *aha2 and aha2 aha7* mutants are longer. (A) Pictures of roots representative for the different Arabidopsis lines lacking AHA proteins and grown on solid Hoagland medium (scale bar = 0.5 mm). (B) The length of root hairs is significantly longer for the *aha2* single and *aha2 aha7* double mutants (n > 1000; ***, $P < 0.0001$; ANOVA with Dunnett's multiple comparison test; error bars show SD). Similar results were obtained in three independent replicates. (C) The number of root hairs per 10 mm of primary root length was similar between lines (n = 30; ANOVA with Dunnett's multiple comparison test; error bars show SD). (d) Growth curves show that root hairs of *aha2* grow faster than wild-type, and root hairs of *aha2 aha7* grow as fast as wild-type, but for a longer period (n ≥ 4; error bars show SEM).

Sussman (2012) who did not observe a growth phenotype of *aha2* mutants grown on control plates. To test another growth condition, we grew the wild-type and the *aha2* mutant in a hydroponic system, where we were able to reproduce the growth phenotype (Fig. S3), which supports the notion that *AHA2* positively, influences seedling growth.

Loss of AHA2 coincides with downregulation of a major potassium uptake system

To analyze if loss of *AHA2* would have an impact on the concentration of K, Fe or P in roots under normal growth conditions, we performed ICP-OES on hydroponically grown *aha2* and wild-type plants. The concentration of

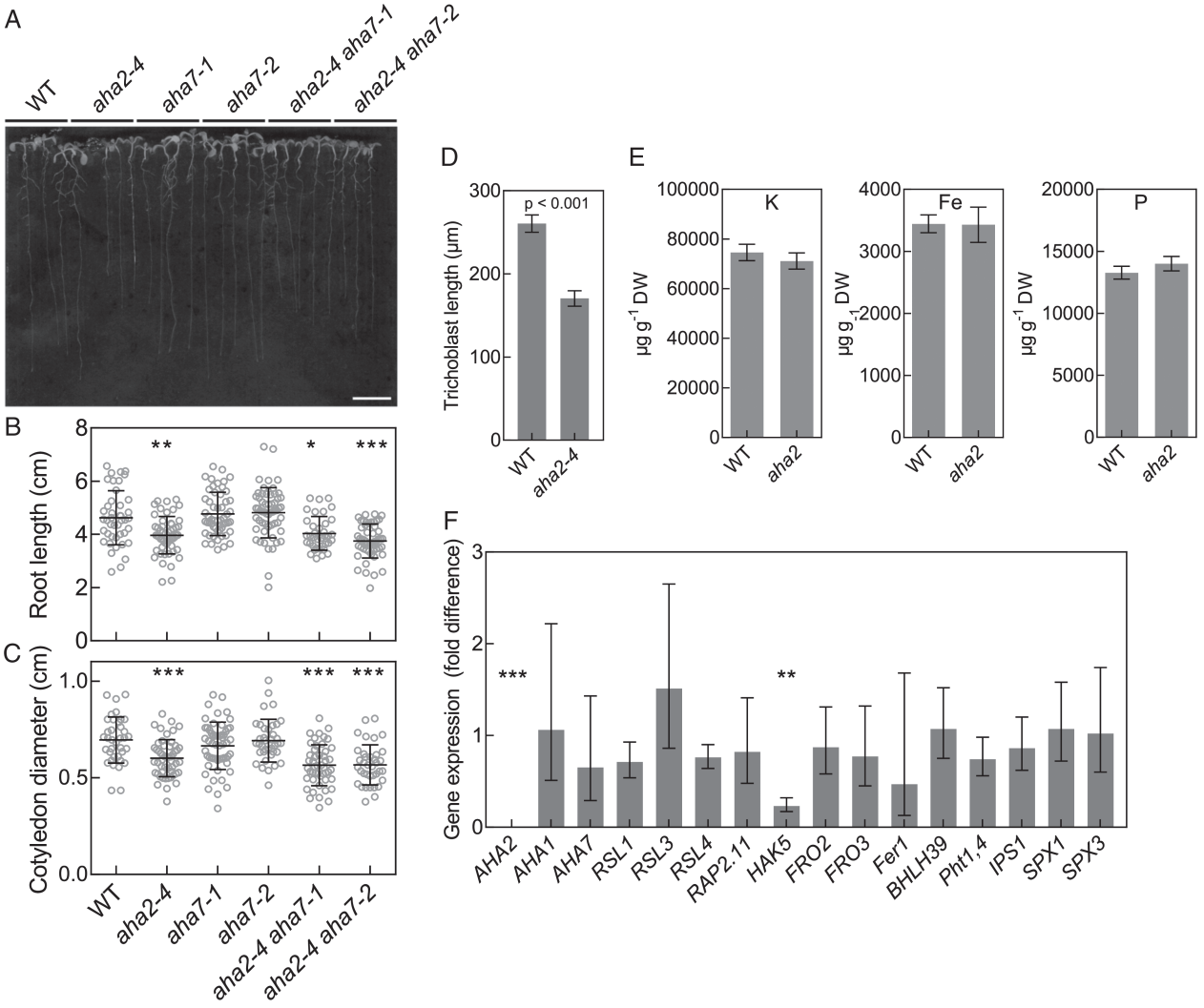

Fig. 4. Loss of *aha2* leads to shorter roots and smaller cotyledons. (A) Representative seedlings grown for 7 days on Hoagland medium (scale bar 1 cm). (B) Root length of *aha2* and *aha2 aha7* double mutants is reduced compared to wild-type, whereas *aha7* single mutant lines are similar to wild-type ($n \geq 35$, $^{**}P < 0.001$, $^{***}P < 0.0001$; ANOVA with Dunnett's multiple comparison test; error bars show SD). (C) Cotyledon diameter of *aha2* and *aha2 aha7* double mutants is reduced compared to wild-type, whereas *aha7* single mutant lines are similar to wild-type ($n \geq 35$, *** $P < 0.001$; ANOVA with Dunnett's multiple comparison test; error bars show SD). (D) Length of trichoblast cells is shorter in *aha2* than wild-type ($n \geq 7$; Student's *t* test; error bars show SD). (E) ICP-OES results show that K, Fe and P are unaltered in roots of hydroponically grown *aha2* compared to wild-type (pool of 16–22 plants, Student's *t* test; error bars show SD). (F) qPCR results show that in 7-day-old roots of *aha2*, *AHA2* itself and *HAK5*, a high affinity potassium uptake protein, are significantly downregulated compared to wild-type ($^{**}P < 0.001$, $^{***}P < 0.0001$; Student's *t* test; error bars show SD). Results are from six biological replicates with around 20 roots each. Genes well known for their responsiveness under altered iron (*FRO2, FRO3, FER1, BHLH39*), phosphate conditions (*PHT1;4, SPX1, SPX3*), transcription factors controlling cell growth and size in root hairs (*RSL1, RSL3, RSL4*) and a transcription factor modulating plant response to low-potassium conditions (*RAP2.11*) were unchanged in *aha2*.

these elements in the wild-type and *aha2* mutant plants was found to be the same (Fig. 4E). Using seedlings grown on plates with Hoagland medium, we tested by qPCR if genes expressed in roots and related to the phosphate starvation response, iron starvation response, potassium uptake or transcription factors controlling cell growth and size in root hairs were differentially regulated. The only gene we found to be differentially expressed was *HAK5*, which was downregulated (Fig. 4F). *HAK5* is a high affinity potassium importer regulating cellular potassium concentration in cells. The *aha2* mutant shows a greatly reduced plasma membrane potential, seen when plants are grown in the presence of toxic hygromycin, which is taken up as a function of the membrane potential (Fig. S4). Thus, depending on the K^+ concentration in the growth medium, *HAK5* may be

downregulated in the absence of *aha2* in order to prevent further membrane depolarization. In the light of this, a possible explanation for the observed reduced growth of trichoblast cells is that, in the absence of *AHA2*, a reduced plasma membrane potential in combination with downregulation of *HAK5* leads to a reduced influx of potassium, which in turn limits water uptake and turgor-driven cell expansion. This is in agreement with the findings that *HAK5* expression is induced by membrane hyperpolarization (K^+ starvation) and reduced by depolarization (NaCl stress; Nieves-Cordones et al. 2008, Rubio et al. 2014). In a transcriptomic study, Haruta and Sussman (2012) reported that *HAK5* was upregulated in the *aha2* background. In this study, whole seedlings, and not just roots, were employed, and the seedlings of both wild-type and *aha2* mutants appeared considerably smaller than those employed in the present study. Whether this can explain the opposing effects on *HAK5* expression levels is currently unknown, but it suggests that K^+ uptake activity coupled with AHA2 function is dynamically regulated, possibly depending on growth conditions, developmental stage or cell types.

Conclusions

In this work, we have shown that AHA7 is a plasma membrane H^+-ATPase with unusual properties. AHA7 is regulated by an autoinhibitory extracellular loop, which secures that the pump only operates under conditions where apoplastic pH is ≥6.0. Furthermore, AHA7 shows half-maximal activity already at neutral cytoplasmic pH, which compared to AHA2 demonstrates a looser control from the cytoplasmic side. We have also shown that AHA2 contributes to root cell expansion already under normal growth conditions, possibly by interfering indirectly with K^+ uptake through the HAK5 transporter. Finally, we observed that AHA2 and AHA7 unexpectedly limit root hair elongation, and that they have different roles in this process.

Author contributions

R.D.H., L.I.O. and M.P. planned the study. All authors contributed to performing the experiments. M.P., R.D.H., J.T.P. and L.I.O. wrote the manuscript. All authors approved the final version.

Acknowledgements – This work was supported by the University of Copenhagen Excellency Program KU2016 and the Innovation Fund Denmark project LESSISMORE.

References

Abascal F, Zardoya R, Posada D (2005) ProtTest: selection of best-fit models of protein evolution. Bioinformatics 21: 2104–2105

Axelsen KB, Palmgren MG (2001) Inventory of the superfamily of P-type ion pumps in Arabidopsis. Plant Physiol 126: 696–706

Axelsen KB, Venema K, Jahn T, Baunsgaard L, Palmgren MG (1999) Molecular dissection of the C-terminal regulatory domain of the plant plasma membrane H^+-ATPase AHA2: mapping of residues that when altered give rise to an activated enzyme. Biochemistry 38: 7227–7234

Baginski ES, Foa PP, Zak B (1967) Microdetermination of inorganic phosphate, phospholipids, and total phosphate in biologic materials. Clin Chem 13: 326–332

Becker JD, Takeda S, Borges F, Dolan L, Feijó JA (2014) Transcriptional profiling of Arabidopsis root hairs and pollen defines an apical cell growth signature. BMC Plant Biol 14: 197

Boavida LC, McCormick S (2007) Temperature as a determinant factor for increased and reproducible in vitro pollen germination in *Arabidopsis thaliana*. Plant J 52: 570–582

Buch-Pedersen MJ, Moller AL, Palmgren MG (2003) Mutagenic study of residues in transmembrane helix 4,5, and 6 of the plant plasma membrane P-type H^+-ATPase. Annual N Y Acad Sci 986: 349–350

Buch-Pedersen MJ, Pedersen BP, Veierskov B, Nissen P, Palmgren MG (2009) Protons and how they are transported by proton pumps. Pflugers Arch 457: 573–579

Certal AC, Almeida RB, Carvalho LM, Wong E, Moreno N, Michard E, Carneiro J, Rodriguéz-Léon J, Wu HM, Cheung AY, Feijó JA (2008) Exclusion of a proton ATPase from the apical membrane is associated with cell polarity and tip growth in Nicotiana tabacum pollen tubes. Plant Cell 20: 614–634

Curtis MD, Grossniklaus U (2003) A gateway cloning vector set for high-throughput functional analysis of genes in planta. Plant Physiol 133: 462–469

Duby G, Boutry M (2009) The plant plasma membrane proton pump ATPase: a highly regulated P-type ATPase with multiple physiological roles. Pflugers Arch 457: 645–655

Edgar RC (2004) MUSCLE: a multiple sequence alignment method with reduced time and space complexity. BMC Bioinformatics 5: 113

Gilroy S, Jones DL (2000) Through form to function: root hair development and nutrient uptake. Trends Plant Sci 5: 56–60

Harper JF, Surowy TK, Sussman MR (1989) Molecular cloning and sequence of cDNA encoding the plasma membrane proton pump (H^+-ATPase) of *Arabidopsis thaliana*. Proc Natl Acad Sci USA 86: 1234–1238

Harper JF, Manney L, DeWitt ND, Yoo MH, Sussman MR (1990) The *Arabidopsis thaliana* plasma membrane H^+-ATPase multigene family. Genomic sequence and

expression of a third isoform. J Biol Chem 265: 13601–13608
Haruta M, Sussman MR (2012) The effect of a genetically reduced plasma membrane protonmotive force on vegetative growth of Arabidopsis. Plant Physiol 158: 1158–1171
Haruta M, Burch HL, Nelson RB, Barrett-Wilt G, Kline KG, Mohsin SB, Young JC, Otegui MS, Sussman MR (2010) Molecular characterization of mutant Arabidopsis plants with reduced plasma membrane proton pump activity. J Biol Chem 285: 17918–17929
Hedrich R, Schroeder JI (1989) The physiology of ion channels and electrogenic pumps in higher plants. Annu Rev Plant Physiol 40: 539–569
Koncz C, Schell J (1986) The promoter of TL-DNA gene 5 controls the tissue-specific expression of chimaeric genes carried by a novel type of Agrobacterium binary vector. Mol Gen Genet 204: 383–336
Lan P, Li W, Lin WD, Santi S, Schmidt W (2013) Mapping gene activity of Arabidopsis root hairs. Genome Biol 14: R67
Le SQ, Gascuel O (1993) An improved general amino acid replacement matrix. Mol Biol Evol 25: 1307–1320
Lin CY, Huang LY, Chi WC, Huang TL, Kakimoto T, Tsai CR, Huang HJ (2015) Pathways involved in vanadate-induced root hair formation in Arabidopsis. Physiol Plant 153: 137–148
Logemann E, Birkenbihl RP, Ülker B, Somssich IE (2006) An improved method for preparing Agrobacterium cells that simplifies the Arabidopsis transformation protocol. Plant Methods 2: 16
Miller MA, Pfeiffer W, Schwartz T (2010) Creating the CIPRES science gateway for inference of large phylogenetic trees. In: Proceedings of the Gateway Computing Environments Workshop (GCE) 14 Nov. 2010, New Orleans, LA, pp 1–8
Młodzińska E, Kłobus G, Christensen MD, Fuglsang AT (2015) The plasma membrane H^+-ATPase AHA2 contributes to the root architecture in response to different nitrogen supply. Physiol Plant 154: 270–282
Monshausen GB, Bibikova TN, Messerli MA, Shi C, Gilroy S (2007) Oscillations in extracellular pH and reactive oxygen species modulate tip growth of Arabidopsis root hairs. Proc Natl Acad Sci U S A 104: 20996–21001
Murashige T, Skoog F (1962) A revised medium for rapid growth and bio assays with tobacco tissue cultures. Physiol Plant 15: 473–497
Nieves-Cordones M, Miller AJ, Alemán F, Martínez V, Rubio F (2008) A putative role for the plasma membrane potential in the control of the expression of the gene encoding the tomato high-affinity potassium transporter HAK5. Plant Mol Biol 68: 521–532
Olsen LI, Hansen TH, Larue C, Østerberg JT, Hoffmann RD, Liesche J, Krämer U, Surblé S, Cadarsi S, Samson VA, Grolimund D, Husted S, Palmgren M (2016) Mother-plant-mediated pumping of zinc into the developing seed. Nat Plants 2: 16036
Palmgren MG (2001) Plant plasma membrane H^+-ATPases: powerhouses for nutrient uptake. Annu Rev Plant Biol 52: 817–845
Palmgren M, Engström K, Hallström BM, Wahlberg K, Søndergaard DA, Säll T, Vahter M, Broberg K (2017) AS3MT-mediated tolerance to arsenic evolved by multiple independent horizontal gene transfers from bacteria to eukaryotes. PLoS One 12: e0175422
Pardo JM, Serrano R (1989) Structure of a plasma membrane H^+-ATPase gene from the plant *Arabidopsis thaliana*. J Biol Chem 264: 8557–8562
Pedersen BP, Buch-Pedersen MJ, Morth JP, Palmgren MG, Nissen P (2007) Crystal structure of the plasma membrane proton pump. Nature 450: 1111–1114
Poole RJ (1978) Energy coupling for membrane transport. Annu Rev Plant Physiol 29: 437–460
Ronquist F, Huelsenbeck JP (2003) MrBayes 3: Bayesian phylogenetic inference under mixed models. Bioinformatics 19: 1572–1574
Rubio F, Fon M, Ródenas R, Nieves-Cordones M, Alemán F, Rivero RM, Martínez V (2014) A low K^+ signal is required for functional high-affinity K^+ uptake through HAK5 transporters. Physiol Plant 152: 558–570
Santi S, Schmidt W (2009) Dissecting iron deficiency-induced proton extrusion in Arabidopsis roots. New Phytol 183: 1072–1084
Schneider CA, Rasband WS, Eliceiri KW (2012) NIH image to ImageJ: 25 years of image analysis. Nat Methods 9: 671–675
Schoenaers S, Balcerowicz D, Vissenberg K (2017) Molecular mechanisms regulating root hair tip growth: A comparison with pollen tubes. In: Obermeyer G, Feijó J (eds) Pollen Tip Growth. Springer, Cham
Sondergaard TE, Schulz A, Palmgren MG (2004) Energization of transport processes in plants. Roles of the plasma membrane H^+-ATPase. Plant Physiol 136: 2475–2482
Tamura K, Stecher G, Peterson D, Filipski A, Kumar S. (2013) MEGA6: Molecular Evolutionary Genetics Analysis version 6.0. Mol Biol Evol 30: 2725–2729
Villalba JM, Palmgren MG, Berberián GE, Ferguson C, Serrano R (1992) Functional expression of plant plasma membrane H^+-ATPase in yeast endoplasmic reticulum. J Biol Chem 267: 12341–12349
Wang H, Inukai Y, Yamauchi A (2007) Root development and nutrient uptake. Crit Rev Plant Sci 25: 279–301
Wielandt AG, Pedersen JT, Falhof J, Kemmer GC, Lund A, Ekberg K, Fuglsang AT, Pomorski TG, Buch-Pedersen MJ, Palmgren M (2015) Specific activation of the plant P-type plasma membrane H^+-ATPase by lysophospholipids depends on the autoinhibitory N- and C-terminal domains. J Biol Chem 290: 16281–16291

Yuan W, Zhang D, Song T, Xu F, Lin S, Xu W, Li Q, Zhu Y, Liang J, Zhang J (2017) Arabidopsis plasma membrane H^+-ATPase genes AHA2 and AHA7 have distinct and overlapping roles in the modulation of root tip H^+ efflux in response to low-phosphorus stress. J Exp Bot 68: 1731–1741

Supporting Information

Additional supporting information may be found online in the Supporting Information section at the end of the article.

Table S1. *aha7* knock out alleles segregate normally.

Table S2. List of primers for genotyping and cloning used in this study.

Table S3. qPCR primers used in this study

Fig. S1. Alignment of the C-terminal regulatory domains of plasma membrane H^+-ATPases.

Fig. S2. Expression of recombinant AHA2 and AHA2 proteins in yeast microsomal membranes.

Fig. S3. Hydroponically grown *aha2* have less biomass than WT.

Fig. S4. Growth with hygromycin shows effects of disturbance in proton motive force.

Edited by J. Schjoerring